



Heat Transfer and Flow Attributes of MHD Viscous Fluid Around a Circular Cylinder in Presence of Thermal Radiation

Bhriгу Kumar Kalita*, Rita Choudhury

Department of Mathematics, Gauhati University, Guwahati, Assam 781014, India

Corresponding Author Email: kumar90bhriгу@gmail.com

<https://doi.org/10.18280/mmep.090106>

ABSTRACT

Received: 26 May 2021

Accepted: 30 November 2021

Keywords:

boundary layer, circular cylinder, heat transfer, magnetohydrodynamic, Nusselt number, skin friction

The crux of this paper is to explore heat distribution and motility traits of electrically conducting viscous fluid around a circular cylinder. The flow is two dimensional and is subjected to magnetic field and thermal radiation. Appropriate numeric computing environment is utilized for numerical solution of the set of transformed differential equations obtained using similarity transformation to the governing equations of the problem. The impinges of physical situation and different flow dictating parameters relevant to the problem have been depicted pictorially in the form of graphs. On the basis of these pictorial visualizations, attempts have been made for inferences regarding the problem. Point of separation is procured with respect to pertinent flow traits.

1. INTRODUCTION

Furtherance in diverse sectors of engineering and technology has been monumentally benefited by the concept of boundary layer approximation. Various production operations viz. extrusion of metal and plastic objects, manufacturing of sticky tapes, cladding of metal or plastic surfaces and so on, utilize the process of thermal boundary layer flow of electrically conducting viscous fluid.

Flow of fluids around a circular cylindrical formation is substantially existent and furnish a wide range of alternatives for practical execution. In particular, hydrodynamic viscous fluid flow in presence of magnetic field and heat transfer has feasible relevance in design of nuclear power plant cooling set-up, heat exchangers, power lines, solar power collector, etc.

Steady magnetohydrodynamic flow around a circular cylinder stands out to be one of the primordial problems that researchers came across regarding circular cylinder. Ingham [1] and Bramley [2] have addressed such problems in their respective studies. Numerical perspective for MHD flow past a circular cylinder has been provided by Raghava Rao and Sekhar [3].

Hydromagnetic flow past a circular cylinder at high Reynolds number have gone under exploration of researchers viz. Kumar and Rajathy [4] and Catalano et al. [5]. Problems of same texture with low and moderate Reynolds numbers have been scrutinized by Kumar and Rajathy [6]. Zhao et al. [7] have executed an exploration on drag characteristic at high Reynolds numbers. Drag and pressure fields for hydromagnetic flow at intermediate Reynolds numbers have been looked into by Sekhar et al. [8].

Dennis et al. [9] and Sen et al. [10] have brought forth solutions for steady separated flow past a circular cylinder at low Reynolds numbers. Steady laminar forced convection at low Reynolds numbers has been diagnosed by Dennis and Chang [11]. Kawaguti [12] have come up with numerical

solution of the Navier-Stokes equations for flow around a circular cylinder at a specific Reynolds number.

Impact of magnetic Reynolds number on hydromagnetic flow past a circular cylinder has been ascertained by Sekhar et al. [13]. Sivakumar et al. [14] have reported ascendancy of induced magnetic field on thermal magnetohydrodynamic flow. Investigation of steady viscous flows past a cylinder have been appraised by a few authors viz. Grove et al. [15], Takami and Keller [16], Hamielec and Raal [17].

A systematic approach to numerical calculation of some essential quantities of two-dimensional flow over a circular cylinder has been furnished by Posdziech and Grundmann [18]. Grigoriadis et al. [19] have used immersed boundary method to procure solution of MHD flow past a circular cylinder. Bovand et al. [20] have discussed the control of flow around cylinder wrapped with porous layer created by magnetohydrodynamic.

Experimental scrutiny on rotating cylinder encompassed within the Eckert number phenomena has been delineated in report of Gschwendtner [21]. Bhattacharyya et al. [22] have considered a hexagonal cylinder and performed numerical simulation of flow and heat transfer mechanism around it.

Heat transmission, incited by thermal radiation, associated with hydromagnetic flow enjoys enactment in gas turbines, nuclear power plants, energy storage system, etc. Hossain et al. [23] and Javed et al. [24] have evaluated thermal radiation effects on convective flow over cylinders.

Point of separation is a crucial aspect in flow around cylinders of different spatial geometries. Along with phenomenological outlook, physical apprehension of point of separation serves as directive for numerous designing or implementation pertaining cylindrical constructions in the domain of civil, hydraulic, mechanical and wind engineering by Zdravkovich [25]. According to Schlichting [26], the exact value of separation point for Newtonian fluid around a circular cylinder is 109.6.

In this study flow and heat transfer attributes of viscous

magnetohydrodynamic fluid around a circular cylinder in presence of thermal radiation have been scrutinized. Furthermore, point of separation has been found out and influence of concomitant parameters on shifting of this point has been monitored.

2. EQUATIONS AND BOUNDARY CONDITIONS

A flow of a viscous fluid around a circular cylinder is taken into consideration. The fluid is incompressible and is electrically conducting. The cylinder is immovable with radius c and kept at a unchanging temperature T_w . Outside the boundary layer at infinity, the fluid is pushing forward with a consistent velocity U_∞ and temperature T_∞ such that $T_w > T_\infty$. Cylindrical polar coordinate system (r, θ, z) emerges naturally for geometrical representation of the problem where convenience is ensured when z-axis coincides with the axis of the cylinder. Thus, fluid flow is two-dimensional along r and θ directions.

It is a matter of amenity to convert the two dimensional coordinates (r, θ) into more familiar Cartesian coordinate system (x, y) with transformations $y = r \sin \theta$ and $x = r \cos \theta$ which in turn converts the governing equations to the following ones:

$$\frac{\partial u}{\partial x} + \frac{\partial v}{\partial y} = 0 \quad (1)$$

$$u \frac{\partial u}{\partial x} + v \frac{\partial u}{\partial y} = \nu \frac{\partial^2 u}{\partial y^2} + U \frac{dU}{dx} + \frac{\sigma B_0^2}{\rho} (U - u) + g \lambda (T - T_\infty) \quad (2)$$

$$u \frac{\partial T}{\partial x} + v \frac{\partial T}{\partial y} = \frac{\mu}{\rho C_p} \left(\frac{\partial u}{\partial y} \right)^2 + \frac{\kappa}{\rho C_p} \frac{\partial^2 T}{\partial y^2} - \frac{1}{\rho C_p} \frac{\partial Q_r}{\partial y} \quad (3)$$

Using the Rosseland approximation for radiation, the radiative heat flux is simplified as:

$$Q_r = -\frac{4\sigma_r}{3k_r} \frac{\partial T^4}{\partial y} \quad (4)$$

With the presumption that temperature differences within the flow exists, the term T^4 can be expressed as a linear function of temperature. On the basis of this premise, expressing T^4 in a Taylor series about T_∞ and neglecting the higher order terms, we arrive at the following approximation:

$$T^4 \cong 4T_\infty^3 T - 3T_\infty^4 \quad (5)$$

In light of Eq. (5), Eq. (4) gives:

$$Q_r = -\frac{16\sigma_r T_\infty^3}{3k_r} \frac{\partial T}{\partial y} \quad (6)$$

Expression in Eq. (6), when incorporated in Eq. (3), we obtain:

$$u \frac{\partial T}{\partial x} + v \frac{\partial T}{\partial y} = \frac{\mu}{\rho C_p} \left(\frac{\partial u}{\partial y} \right)^2 + \frac{\kappa}{\rho C_p} \frac{\partial^2 T}{\partial y^2} + \frac{1}{\rho C_p} \frac{16\sigma_r T_\infty^3}{3k_r} \frac{\partial^2 T}{\partial y^2} \quad (7)$$

Thus Eq. (1), Eq. (2) and Eq. (7) constitute the system of governing equations of the problem under consideration.

The germane boundary conditions are,

$$y = 0 : u = 0, v = 0, T = T_w \quad (8)$$

$$y \rightarrow \infty : u \rightarrow U, T \rightarrow T_\infty \quad (9)$$

The mainstream velocity U and the stream-function ϕ are given by,

$$U(\theta) = 2U_\infty \sin \theta \quad (10)$$

$$\phi = \sqrt{2cU_\infty \nu} \left\{ \frac{\theta}{1!} g_1(\xi) - \frac{4}{3!} \theta^3 g_3(\xi) + \frac{6}{5!} \theta^5 g_5(\xi) - \frac{8}{7!} \theta^7 g_7(\xi) + \dots \right\} \quad (11)$$

where, $\xi = y \sqrt{\frac{2U_\infty}{c\nu}}$

With the help of stream-function the velocity components are given as:

$$u = \frac{\partial \phi}{\partial y} = 2U_\infty \left\{ \frac{\theta}{1} g_1'(\xi) - \frac{2}{3} \theta^3 g_3'(\xi) + \frac{1}{20} \theta^5 g_5'(\xi) - \frac{1}{630} \theta^7 g_7'(\xi) + \dots \right\} \quad (12)$$

$$v = -\frac{\partial \phi}{\partial x} = -\sqrt{\frac{2\nu U_\infty}{c}} \left\{ \frac{1}{1!} g_1(\xi) - 2\theta^2 g_3(\xi) + \frac{1}{4} \theta^4 g_5(\xi) - \frac{1}{90} \theta^6 g_7(\xi) + \dots \right\} \quad (13)$$

The temperature within the thermal boundary layer is given by:

$$\beta = \frac{T - T_\infty}{T_w - T_\infty} = 4E \left\{ h_1(\xi) - \theta^2 h_3(\xi) + \theta^4 h_5(\xi) - \theta^6 h_7(\xi) + \dots \right\} \quad (14)$$

where, $E = \frac{U_\infty^2}{c_p(T_w - T_\infty)}$ is the Eckert number.

Clearly temperature given by β is dimensionless but u, v are not. So, it is customary to consider $u^* = \frac{u}{2U_\infty}$ and $v^* =$

$\sqrt{\frac{c}{2\nu U_\infty}}$ v as non-dimensional velocity components.

To avoid complexity of succeeding calculative procedures, it would be authentic to neglect terms $g_n(\xi), g_n'(\xi), h_n(\xi)$ for $n \geq 9$.

The boundary conditions, in terms of $g_n(\xi), g_n'(\xi), h_n(\xi)$ for $n = 1, 3, 5, 7$, are:

$$\begin{aligned} \xi = 0 : g_n = 0, g'_n = 0, \\ h_1 = \frac{1}{4E}, h_3 = h_5 = h_7 = 0 \end{aligned} \quad (15)$$

$$\begin{aligned} \xi \rightarrow \infty : g'_1 \rightarrow 1, g'_3 \rightarrow \frac{1}{4}, \\ g'_5 \rightarrow \frac{1}{6}, g'_7 \rightarrow \frac{1}{8}, h_n \rightarrow 0 \end{aligned} \quad (16)$$

Now, picking up the values of u , v and T from Eqns. (12)-(14) and substituting in Eq. (1), Eq. (2) and Eq. (7), we equate the like powers of θ on both sides of the equations to get the following set of equations.

$$g_1''' + g_1 g_1'' - g_1'^2 - M g_1' + G_r E h_1 + M + 1 = 0 \quad (17)$$

$$\begin{aligned} g_3''' + g_1 g_3'' + 3 g_3' g_3' - 4 g_1' g_3' \\ + \frac{3}{2} E G_r h_3 - M g_3' + \frac{M}{4} + 1 = 0 \end{aligned} \quad (18)$$

$$\begin{aligned} g_5''' + g_1 g_5'' + 5 g_5' g_3' - 6 g_1' g_5' - M g_5' - \frac{80}{3} (g_3')^2 \\ + \frac{80}{3} g_3' g_3'' + 20 E G_r h_5 + \frac{M}{6} + \frac{8}{3} = 0 \end{aligned} \quad (19)$$

$$\begin{aligned} g_7''' + g_1 g_7'' + 7 g_7' g_3' - 8 g_1' g_7' + 63 g_3' g_5' - M g_7' \\ + 105 g_3' g_5' - 168 g_3' g_5' + 630 E G_r h_7 + \frac{M}{8} + 8 = 0 \end{aligned} \quad (20)$$

$$h_1'' + \left(\frac{P_r}{1+R} \right) g_1 h_1' = 0 \quad (21)$$

$$\begin{aligned} h_3'' + \left(\frac{P_r}{1+R} \right) \{ g_1 h_3' - 2 g_1' h_3 \\ + 2 g_3 h_1' - (g_1')^2 \} = 0 \end{aligned} \quad (22)$$

$$\begin{aligned} h_5'' + \left(\frac{P_r}{1+R} \right) \{ g_1 h_5' - 4 g_1' h_5 + 2 g_3 h_3' \\ - \frac{4}{3} g_3' h_3 + \frac{1}{4} g_5 h_1' - \frac{4}{3} g_1' g_3'' \} = 0 \end{aligned} \quad (23)$$

$$\begin{aligned} h_7'' + \left(\frac{P_r}{1+R} \right) \{ g_1 h_7' - 6 g_1' h_7 + 2 g_3 h_5' \\ - \frac{8}{3} g_3' h_5 + \frac{1}{4} g_5 h_3' - \frac{1}{10} g_5' h_3 + \frac{1}{90} g_7 h_1' \\ - \frac{1}{10} g_1' g_5'' - \frac{4}{9} (g_3')^2 \} = 0 \end{aligned} \quad (24)$$

where, $M = \frac{\sigma B_0^2 c}{2 U_\infty \rho}$, $P_r = \frac{\rho v C_p}{\kappa}$, $R = \frac{16 \sigma_r T_\infty^3}{3 k_r \kappa}$ and $G_r = \frac{g \lambda (T_s - T_\infty) c^2}{U_\infty^2 x}$ are magnetic parameter, Prandtl number, thermal radiation parameter and Grashof number for heat transfer, respectively.

Skin friction in its dimensionless form is given by:

$$\begin{aligned} S_f = \frac{\left(\frac{\partial u}{\partial y} \right)_{y=0}}{2 \rho U_\infty \sqrt{\frac{2 \nu U_\infty}{c}}} = \left\{ \frac{\theta}{1} g_1''(\xi) \right. \\ \left. - \frac{2}{3} \theta^3 g_3''(\xi) + \frac{1}{20} \theta^5 g_5''(\xi) - \frac{1}{630} \theta^7 g_7''(\xi) \right\}_{\xi=0} \end{aligned} \quad (25)$$

Heat flux in terms of Nusselt number is given by:

$$\begin{aligned} Nu = - \frac{c \left(\frac{\partial T}{\partial y} \right)_{y=0}}{(T_w - T_\infty)} = -4 E \sqrt{Re} \{ h_1'(\xi) \\ - \theta^2 h_3'(\xi) + \theta h_4'(\xi) - \theta^6 h_7'(\xi) \}_{\xi=0} \end{aligned} \quad (26)$$

Here $Re = \frac{2 U_\infty c}{\nu}$ is Reynolds number. For suitability of representation, we define $N_u = \frac{Nu}{\sqrt{Re}}$.

3. SOLUTION OF THE PROBLEM

The set of Eqns. (17)-(24), in the light of boundary conditions represented by Eq. (15) and Eq. (16), have been solved numerically using bvp4c solver incorporated in MATLAB.

4. RESULTS AND DISCUSSION

In light of graphical outline of the numerical computations, influences of some flow parameters on fluid motility and heat transportation mechanism have been perceived. The gist of this study has summed up influence of magnetic parameter, thermal radiation parameter, Prandtl number and Grashof number on germane flow attributes and thermal indicatives. Unless otherwise stated, this evaluation has been executed with numeric values of the parameters as $M=0.02$, $E=0.001$, $R=0.6$, $P_r=2.4$, $G_r=0.1$.

Depiction of fluctuations in temperature field have been exhibited in Figures 1-10. Figures 1-8 showcase the impact of apropos parameters on heat transmission at various positions of θ . Figure 9 points out the influence of θ with fixed numeric values of parameters. A comprehensive three dimensional visualization of the heat distribution of the flow has been demonstrated in Figure 10.

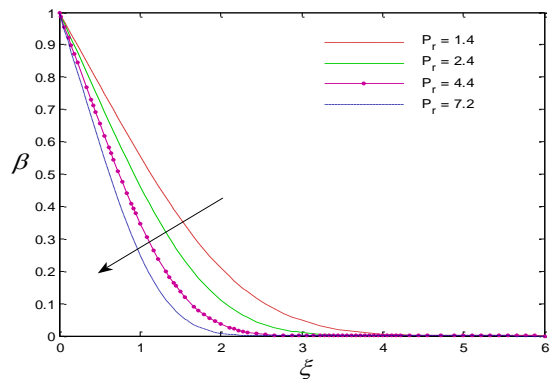


Figure 1. Temperature at $\theta = \frac{\pi}{3}$ for P_r

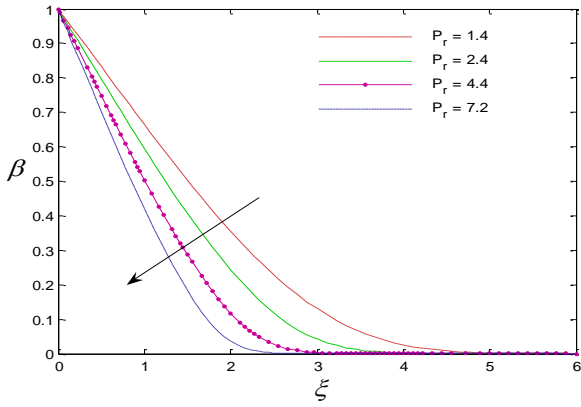


Figure 2. Temperature at $\theta = \frac{\pi}{2}$ for P_r

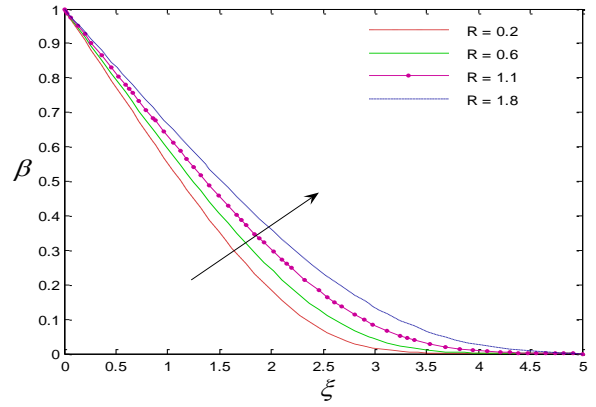


Figure 5. Temperature at $\theta = \frac{\pi}{2}$ for R

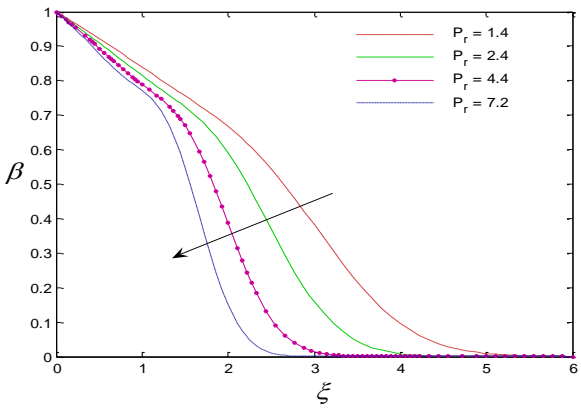


Figure 3. Temperature at $\theta = \frac{2\pi}{3}$ for P_r

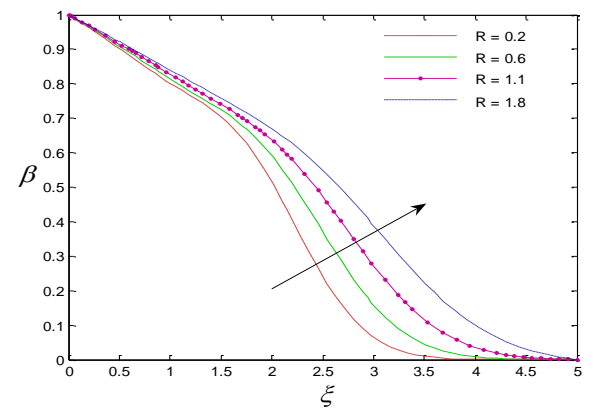


Figure 6. Temperature at $\theta = \frac{2\pi}{3}$ for R

Figures 1-3 elucidate influence of Prandtl number on the temperature field along normal direction at some positions of the cylinder surface viz. $\theta = \frac{\pi}{3}, \frac{\pi}{2}, \frac{2\pi}{3}$. From each of these figures, it is observed that thriving values of Prandtl number impart retarding effect on fluid temperature. It is evident from the fact that a boost in value of Prandtl number retards thermal diffusivity in comparison with momentum diffusivity of the fluid and hence the diminution in temperature is observed.

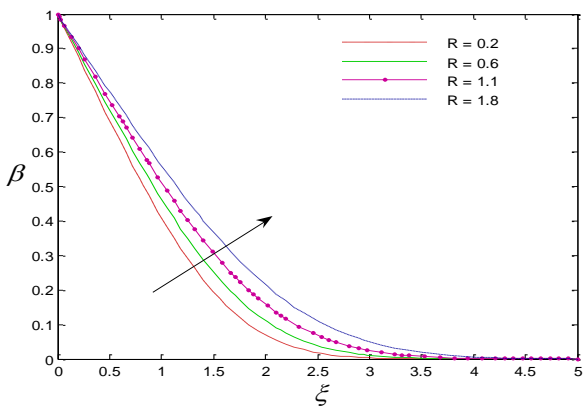


Figure 4. Temperature at $\theta = \frac{\pi}{3}$ for R

Escalation in fluid temperature with intensification of thermal radiation parameter, at $\theta = \frac{\pi}{3}, \frac{\pi}{2}, \frac{2\pi}{3}$, can be noticed from Figures 4-6, respectively. Upsurge in thermal radiation parameter ensures additional quanta of heat input to the flow. As a result, temperature of the fluid gets enhanced.

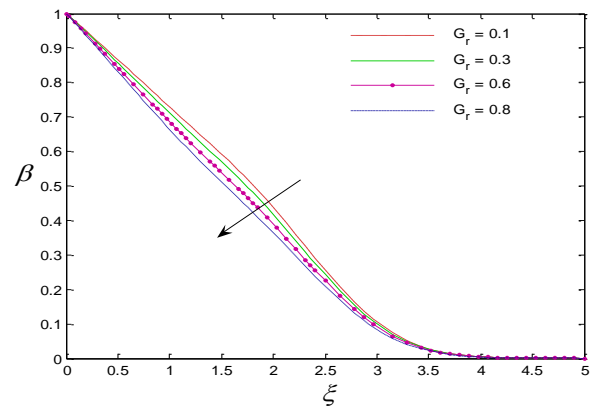


Figure 7. Temperature for G_r at $\theta = \frac{11\pi}{18}$

Augmentation in thermal Grashof number shows hindering effect on fluid temperature as delineated in Figure 7 and Figure 8. Numeric growth in thermal Grashof number encourages weakening of intermolecular binding of fluid particles resulting into strengthening of buoyancy force as opposed to restraining viscous force. Greater buoyancy indicates increase in spatial diffusion which in turn inflicts erosion of heat to the surrounding and thus diminution of temperature is manifested.

Figure 9 outlines the effectiveness of variable θ on thermal condition of the flow mechanism. Facile observation guides to the inference that with increment in θ fluid temperature shoots up. In other words, warmth of the flow intensifies in the direction of fluid flow. Locomotion of the fluid particles transport heat in the direction of flow and consequently, bring

about accumulation of thermal energy towards the backward stagnation point.

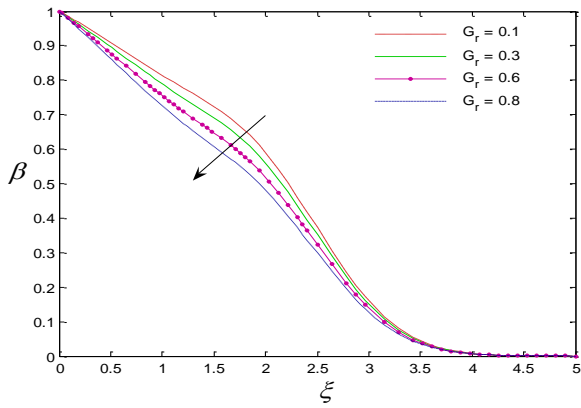


Figure 8. Temperature for G_r at $\theta = \frac{2\pi}{3}$

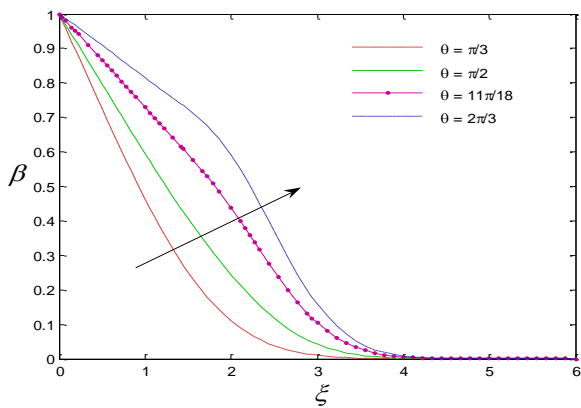


Figure 9. Temperature for θ .

A three dimensional outlook to the temperature profile is furnished in Figure 10. The surface depicted in Figure 10 outlines the pattern of heat distribution $\beta = \beta(\theta, \xi)$.

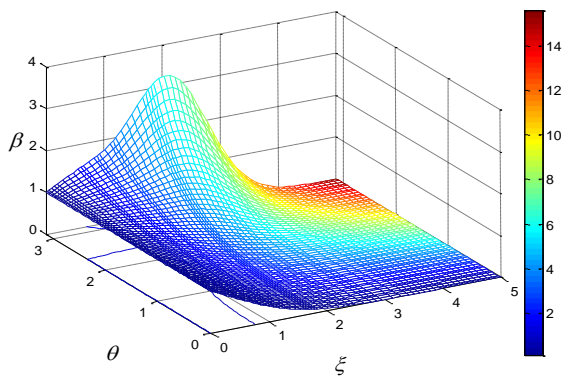


Figure 10. Temperature against (θ, ξ)

Effect of concomitant parameters on Nusselt number is corroborated by Figures 11-14. The profile of Nusselt number shows gradual decline against θ suggesting that heat flux dwindles along the direction of the fluid flow. During the initial phase of the flow i.e. near the forward stagnation point the locomotion of fluid particles at the surface disseminates thermal energy more faster than that in case of downstream flow. Figures 11-13, assist to grasp the fact that upsurge in

magnetic parameter, thermal radiation parameter and Grashof number inflicts growth in Nusselt number. Enhancement in Nusselt number signifies higher rate of heat transfer into the thermal environment of the fluid at the surface of the cylinder. Therefore, strengthened magnetic parameter, thermal radiation parameter and Grashof number induces greater heat dispersion from cylinder surface into the fluid. However, stepping up of Prandtl number instigates hindering effect on Nusselt number as outlined in Figure 14. Strengthened value of Prandtl number evince shrinkage of thermal diffusion as compared to momentum diffusion and consequently, there is descent in Nusselt number.

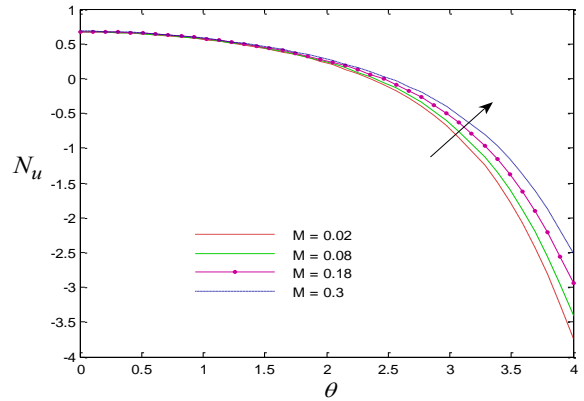


Figure 11. Nusselt number for M

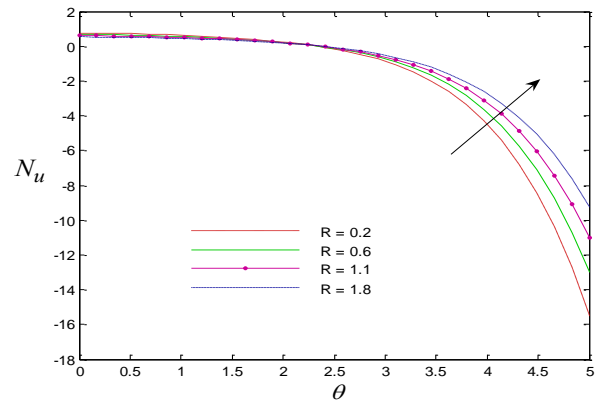


Figure 12. Nusselt number for R

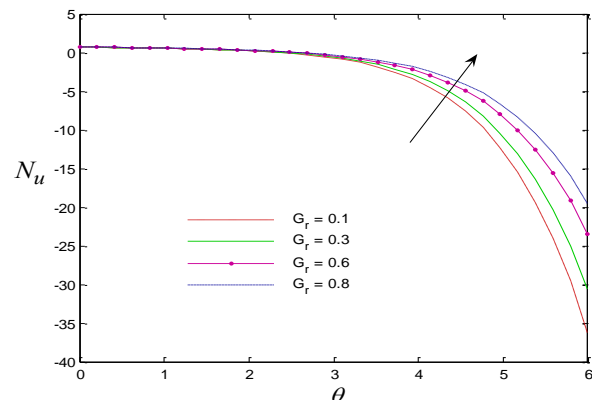


Figure 13. Nusselt number for G_r

Figure 15 and Figure 16 exhibit influence of magnetic parameter and thermal Grashof number on skin friction. It is observed that for a specific magnetic parameter or Grashof number, skin friction expresses slight gain when it leaves

behind the forward stagnation point and after hovering around positive value, subsides precipitously moving towards the backward stagnation point. The central takeaway from Figure 15 and Figure 16 is that escalating value of magnetic parameter or Grashof number results into elevation of skin friction coefficient.

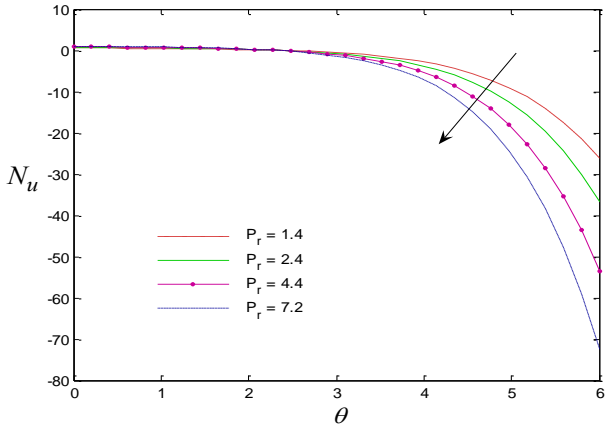


Figure 14. Nusselt number for P_r

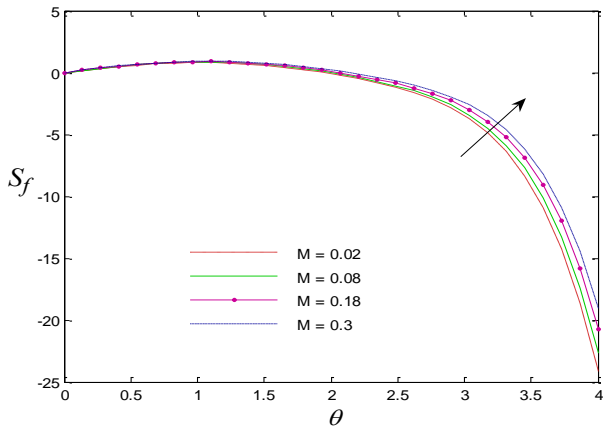


Figure 15. Skin friction for M

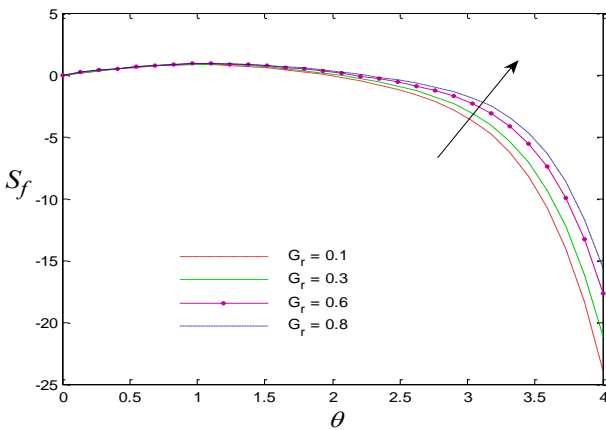


Figure 16. Skin friction for G_r

Point of separation is a prominent observation concomitant to the problem of flow past a circular cylinder. It is conceptualized as the point between forward and backward stagnation points at which the boundary layer gets detached resulting into a stir as depicted in Figure 17. It is given by the non-zero value θ_s of θ for which skin friction coefficient vanishes. Setting $S_f=0$ in Eq. (25) we get the condition for locating the point of separation.

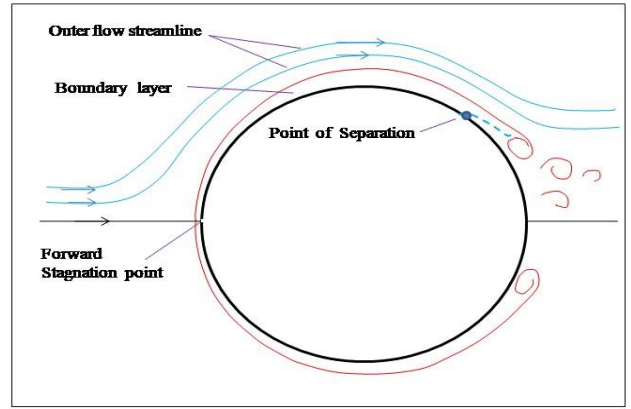


Figure 17. Frame diagram showing point of separation

$$g_1''(0) - \frac{2}{3} g_3''(0) \alpha + \frac{1}{20} g_5''(0) \alpha^2 - \frac{1}{630} g_7''(0) \alpha^3 = 0 \quad (27)$$

where, $\alpha = \theta^2$.

For each value of magnetic parameter or Grashof number, `bvp4c` returns a particular set of values of $g_n''(0)$, $n = 1, 3, 5, 7$. For this reason, Eq. (27) represents a specific cubic equation for each of them. Solving each of such equation, we extract the admissible value of α which in turn gives the value of θ_s .

Table 1. Point of separation for various values of magnetic parameter M with $G_r=0$

M	θ_s in radian	θ_s in degree
0	1.9104	109.46
0.01	1.9170	109.84
0.02	1.9236	110.21
0.08	1.9627	112.45
0.18	2.0262	116.09

Note: It is a matter of convenience to visualize point of separation in degree unit along with radian.

Table 1 and Table 2 display the values of point of separation for different values of magnetic parameter and thermal Grashof number, respectively. It is apparent from the data that intensification of magnetic parameter pushes separation point towards the backward stagnation point. Identical inference can be made in case of impact of Grashof number on point of separation.

Table 2. Point of separation for various values of Grashof number G_r with $M=0$

G_r	θ_s in radian	θ_s in degree
0	1.9104	109.46
0.1	1.9355	110.89
0.3	1.9884	113.93
0.6	2.0757	118.93
0.8	2.1408	122.66

5. CONCLUSIONS

The present work pertaining to heat transfer and locomotion of viscous magnetohydrodynamic fluid flow past a circular cylinder divulges some enthralling inferences.

It is observed that magnetic parameter and thermal Grashof number inflict flourishing consequence on fluid shear rate. The point of separation, in ideal state of affairs characterized by $M=G_r=0$, has turned out to be 109.46° . It is worth mentioning that Schlichting [24] inferred 109.6° to be the precise value of separation point for Newtonian flow past a circular cylinder. Skin friction thrives with the escalation of magnetic parameter which in turn plunges the point of separation towards the backward stagnation point. Similar sort of deduction is applicable to the role of Grashof number in repositioning of separation point.

Heat transfer mechanism gets eminently influenced by concomitant flow parameters. Augmentation in Prandtl number and thermal Grashof number inflict a diminution in warmth of the fluid. However, intensification of thermal radiation parameter encourages escalation of fluid temperature. An additional takeaway is that heat accumulation grows consistently in the direction of flow.

Nusselt number dwindles with an upsurge in value of Prandtl number but shows escalation with the growth of thermal radiation parameter, magnetic parameter and Grashof number. As we move forward along the surface of the cylinder, Nusselt number shows retarding trend.

ACKNOWLEDGMENT

This work is supported financially by University Grants Commission of India.

REFERENCES

- [1] Ingham, D.B. (1974). Steady magnetohydrodynamic flow past a circular cylinder. *International Journal for Numerical Methods in Engineering*, 8(4): 771-781. <https://doi.org/10.1002/nme.1620080407>
- [2] Bramley, J.S. (1974). Magnetohydrodynamic flow past a circular cylinder. *Zeitschrift für angewandte Mathematik und Physik ZAMP*, 25(3): 409-416. <http://doi.org/10.1007/bf01594957>
- [3] Raghava Rao, C.V., Sekhar, T.V.S. (2000). MHD flow past a circular cylinder—A numerical study. *Computational Mechanics*, 26(5): 430-436. <https://doi.org/10.1007/s004660000191>
- [4] Kumar, H., Rajathy, R. (2013). MHD flow past a circular cylinder at high Reynolds numbers. *IUP Journal of Mechanical Engineering*, 6(4): 7-28.
- [5] Catalano, P., Wang, M., Iaccarino, G., Moin, P. (2003). Numerical simulation of the flow around a circular cylinder at high Reynolds numbers. *International Journal of Heat and Fluid Flow*, 24(4): 463-469. [https://doi.org/10.1016/S0142-727X\(03\)00061-4](https://doi.org/10.1016/S0142-727X(03)00061-4)
- [6] Kumar, H., Rajathy, R. (2007). Numerical study of MHD flow past a circular cylinder at low and moderate Reynolds numbers. *International Journal for Computational Methods in Engineering Science and Mechanics*, 7: 461-473. <https://doi.org/10.1080/15502280600790553>
- [7] Zhao, M., Mao, J., Xi, Y.H. (2015). Research on drag characteristic of flow around finite circular cylinder at high Reynolds numbers. *Journal of Mechanical Engineering*, 51(22): 176-182. <http://dx.doi.org/10.3901/JME.2015.22.176>
- [8] Sekhar, T.V.S., Sivakumar, R., Kumar, T.V.R. (2005). Drag and pressure fields for the MHD flow around a circular cylinder at intermediate Reynolds numbers. *Journal of Applied Mathematics*, 2005(3): 183-203. <http://doi.org/10.1155/JAM.2005.183>
- [9] Dennis, S.C.R., Hudson, J.D., Smith, N. (1968). Steady laminar forced convection from a circular cylinder at low Reynolds numbers. *The Physics of Fluids*, 11(5): 933-940. <https://doi.org/10.1063/1.1692061>
- [10] Sen, S., Mittal, S., Biswas, G. (2009). Steady separated flow past a circular cylinder at low Reynolds numbers. *Journal of Fluid Mechanics*, 620: 89-119. <http://doi.org/10.1017/S0022112008004904>
- [11] Dennis, S.C.R., Chang, G.Z. (1970). Numerical solutions for steady flow past a circular cylinder at Reynolds numbers up to 100. *Journal of Fluid Mechanics*, 42(3): 471-489. <https://doi.org/10.1017/S0022112070001428>
- [12] Kawaguti, M. (1953). Numerical solution of the Navier-Stokes equations for the flow around a circular cylinder at Reynolds number 40. *Journal of the Physical Society of Japan*, 8(6): 747-757. <https://doi.org/10.1143/JPSJ.8.747>
- [13] Sekhar, T.V.S., Sivakumar, R., Ravi Kumar, T.V.R. (2009). Effect of magnetic Reynolds number on the two-dimensional hydromagnetic flow around a cylinder. *International Journal for Numerical Methods in Fluids*, 59(12): 1351-1368. <http://doi.org/10.1002/fld.1870>
- [14] Sivakumar, R., Vimala, S., Sekhar, T.V.S. (2015). Influence of induced magnetic field on thermal MHD flow. *Numerical Heat Transfer, Part A: Applications*, 68(7): 797-811. <http://doi.org/10.1080/10407782.2014.994438>
- [15] Grove, A.S., Shair, F.H., Petersen, E.E. (1964). An experimental investigation of the steady separated flow past a circular cylinder. *Journal of Fluid Mechanics*, 19(1): 60-80. <https://doi.org/10.1017/S0022112064000544>
- [16] Takami, H., Keller, H.B. (1969). Steady two-dimensional viscous flow of an incompressible fluid past a circular cylinder. *The Physics of Fluids*, 12(12): II-51. <https://doi.org/10.1063/1.1692469>
- [17] Hamielec, A.E., Raal, J.D. (1969). Numerical studies of viscous flow around circular cylinders. *The Physics of Fluids*, 12(1): 11-17. <https://doi.org/10.1063/1.1692253>
- [18] Posdziech, O., Grundmann, R. (2007). A systematic approach to the numerical calculation of fundamental quantities of the two-dimensional flow over a circular cylinder. *Journal of Fluids and Structures*, 23(3): 479-499. <https://doi.org/10.1016/j.jfluidstructs.2006.09.004>
- [19] Grigoriadis, D.G.E., Sarris, I.E., Kassinos, S.C. (2010). MHD flow past a circular cylinder using the immersed boundary method. *Computers & Fluids*, 39(2): 345-358. <http://doi.org/10.1016/j.compfluid.2009.09.012>
- [20] Bovand, M., Rashidi, S., Esfahani, J.A., Saha, S.C., Gu, Y., Dehesht, M. (2016). Control of flow around a circular cylinder wrapped with a porous layer by magnetohydrodynamic. *Journal of Magnetism and Magnetic Materials*, 401: 1078-1087. <https://doi.org/10.1016/j.jmmm.2015.11.019>
- [21] Gschwendtner, M.A. (2004). The Eckert number phenomenon: Experimental investigations on the heat transfer from a moving wall in the case of a rotating cylinder. *Heat and Mass Transfer*, 40(6): 551-559. <https://doi.org/10.1007/s00231-003-0437-9>

[22] Bhattacharyya, S., Das, S., Sarkar, A., Guin, A., Mullick, A. (2017). Numerical simulation of flow and heat transfer around hexagonal cylinder. *International Journal of Heat and Technology*, 35(2): 360-363. <https://doi.org/10.18280/ijht.350218>

[23] Hossain, M.A., Alim, M.A., Rees, D.A.S. (1998). Effect of thermal radiation on natural convection over cylinders of elliptic cross section. *Acta Mechanica*, 129(3): 177-186. <https://doi.org/10.1007/BF01176744>

[24] Javed, T., Mustafa, I., Ahmad, H. (2017). Effect of thermal radiation on unsteady mixed convection flow near forward stagnation point over a cylinder of elliptic cross section. *Thermal Science*, 21(1 Part A): 243-254. <https://doi.org/10.2298/TSCI140926027J>

[25] Zdravkovich, M.M. (1997). Flow around circular cylinders; vol. I fundamentals. *Journal of Fluid Mechanics*, 350(1): 377-378.

[26] Schlichting, H. (1968). *Boundary Layer Theory*. McGraw Hill, New York.

NOMENCLATURE

c	radius of circular cylinder, m
B_0	magnetic flux density, Wb.m^{-2}
C_p	specific heat at constant pressure, $\text{J.kg}^{-1}.\text{K}^{-1}$
E	Eckert number
$g_i, i = 1, 3, ..$	non dimensional stream functions
$h_i, i = 1, 3, ..$	non dimensional energy functions
k_r	mean absorption coefficient, m^{-1}
M	magnetic parameter
N_u	modified Nusselt number
Nu	Nusselt number
P_r	Prandtl number
Q_r	radiative heat flux, W.m^{-2}
r	radial distance in cylindrical coordinates, m

R	thermal radiation parameter
Re	Reynolds number
S_f	skin friction.
T	fluid temperature, K
T_w	temperature of cylinder, K.
T_∞	fluid temperature at infinity, K
u, v	velocity components, m.s^{-1}
u^*, v^*	non dimensional velocity components
U	stream velocity, m.s^{-1}
U_∞	fluid velocity at infinity, m.s^{-1}
x, y	rectangular coordinates, m
z	height in cylindrical coordinates, m

Greek symbols

β	non dimensional temperature
θ	azimuth in polar or cylindrical coordinates
θ_s	separation point
κ	thermal conductivity, $\text{W.m}^{-1}.\text{K}^{-1}$
μ	dynamic viscosity, $\text{kg.m}^{-1}.\text{s}^{-1}$
ν	kinematic viscosity, $\text{m}^2.\text{s}^{-1}$
ζ	dimensionless variable
ρ	fluid density, kg.m^{-3}
σ	electric conductivity, S.m^{-1} or $\text{kg}^{-1}.\text{m}^{-3}.\text{s}^3.\text{A}^2$
σ_r	Stefan-Boltzmann constant, $\text{W.m}^{-2}.\text{K}^{-4}$
φ	stream function

Subscript

w	surface condition
∞	infinity condition

Superscript

'	derivative with respect to ζ
---	------------------------------------